RESEARCH ARTICLE

Performance assessment of drop tube reactor for biomass fast pyrolysis using process simulator

Fekadu Mosisa Wako[1] | **Gianmaria Pio**[1] | **Ashraf Lofti**[2,3] |
Ernesto Salzano[1] | **Azharuddin Farooqui**[2,3] | **Nader Mahinpey**[2]

[1]Dipartimento di Ingegneria Civile, Chimica, Ambientale e dei Materiali, Università di Bologna, Bologna, Italy

[2]Department of Chemical and Petroleum Engineering, School of Engineering, University of Calgary, Calgary, Alberta, Canada

[3]Nanos Technology and Innovations LTD, Calgary, Alberta, Canada

Correspondence
Nader Mahinpey, Department of Chemical and Petroleum Engineering, School of Engineering, University of Calgary, 2500 University Drive NW, Calgary, AB T2N 1N4, Canada.
Email: nader.mahinpey@ucalgary.ca

Abstract

Biomass pyrolysis process from a drop tube reactor was modelled in a plug flow reactor using Aspen Plus process simulation software. A kinetic mechanism for pyrolysis was developed considering the recent improvements and updated kinetic schemes to account for different content of cellulose, hemicellulose, and lignin. In this regard, oak, beechwood, rice straw, and cassava stalk biomasses were analyzed. The main phenomena governing the pyrolysis process are identified in terms of the characteristic times. Pyrolysis process was found to be reaction rate controlled. Effects of pyrolysis temperature on bio-oil, gases, and char yields were evaluated. At optimum pyrolysis conditions (i.e., 500°C), a bio-oil yield of 67.3, 64, 43, and 52 wt.% were obtained from oak, beechwood, rice straw, and cassava stalk, respectively. Oak and beechwood were found to give high yields of bio-oil, while rice straw produced high gas and char yields compared to other biomasses. Although temperature is the main factor that plays a key role in the distribution of pyrolysis products, the composition of cellulose, hemicellulose, and lignin in the feedstock also determines the yield behaviour and composition of products. With the rise in pyrolysis temperature, further decomposition of intermediate components was initiated favouring the formation of lighter fractions. Comparably, species belonging to the aldehyde chemical family had the highest share of bio-oil components in all the investigated feedstocks. Overall, the present study shows a good agreement with the experimental study reported in the literature, confirming its validity as a predictive tool for the biomass pyrolysis process.

KEYWORDS
Aspen Plus, biomass, bio-oil, pyrolysis, reactor modelling

1 | INTRODUCTION

Currently, fossil fuels are the main source of energy, accounting for about 40% of global energy demand.[1]

However, the rapid consumption of such fuels as well as the composition of burned mixtures lead to serious energy security and environmental issues,[2] thus requiring the adoption of alternative clean energy sources.

Biomass is one of the most promising feedstocks to meet the growing demand for clean energy while satisfying strict environmental regulations. Biomass is a carbon-neutral energy source that can be converted into gaseous fuels via gasification or liquid fuels via pyrolysis.[1] Unluckily, industrial scale-up of biomass conversion is challenging owing to the complexity of its chemistry and transport phenomena involved in the process.[3] For instance, the heat transfer and reaction rates during biomass conversion are strongly influenced by biomass composition and reactor configuration, thereby affecting yield profiles.[4,5] So, biomass conversion requires a deeper understanding of how the feed decomposed, intermediate species consumed, and desired products are produced, via a robust kinetic mechanism.[6] Due to the multi-phase nature of biomass, and the multi-step and multi-scale nature of processing methods, developing an accurate kinetic model is however a challenging step.[7] More specifically, the main efforts in biomass pyrolysis simulation lie in accurately capturing the molecular conversion kinetics.[8]

Several kinetic schemes have been developed in the literature ranging from simple single-step kinetic models to complex reaction models containing hundreds of reactions.[6,9–14] In this light, simplified reaction schemes are reported to be suitable.[15] Pyrolysis is one of the main thermochemical conversion pathways for converting biomass into different chemical components.[16] For the sake of application, these components are usually lumped into bio-oil, gas, and char.[15]

Modelling of biomass pyrolysis typically considers decomposition and devolatilization of the three independent components: cellulose (CELL), hemicellulose (HCE), and lignin.[17] Indeed, the large variability in chemical composition of biomasses promotes the definition of surrogate mixtures suitable for mimicking the real behaviour of a more complex mixture. For these reasons, a detailed kinetic model for pure CELL, HCE, and lignin or their mixtures can be intended as per a robust feature for the evaluation of the chemistry of biomasses. Several studies have been reported on biomass pyrolysis kinetics, including the first global kinetic scheme developed by Shafizadeh et al.[18] where CELL decomposition is represented by three parallel reactions forming active CELL, gases, and char. Active CELL further depolymerizes forming volatile species as reported by Shafizadeh et al.[18] and of which levoglucosan (LVG) is the main fraction.[19] Extensive studies on CELL pyrolysis and its dependence on temperature[20–24] support the assumption that hydroxy acetaldehyde (HAA) is the primary decomposition product, especially through a ring scission reaction that becomes increasingly crucial at elevated temperatures. Piskorz et al.[25] proposed the modified version of the Shafizadeh et al.[18] mechanism, taking into account the formation of both HAA and LVG during CELL pyrolysis. The initial stage of the mechanism considered the competitive formation of char and activated CELL, followed by ring cleavage producing HAA and depolymerization leading to LVG.[25] Later studies[26–28] largely confirm the mechanistic findings of Piskorz et al.[25] Given the heterogeneity of HCE, xylan has been widely considered as a surrogate for understanding the kinetics of HCE pyrolysis.[29–31] Insights between pyrolysis product distribution and structural features of xylose-based HCEs have been reported.[32,33] As described in Ranzi et al.,[6] pyrolysis model, xylose degrades forming two intermediate species (HCE1 and HCE2), followed by successive decomposition routes leading to the formation of xylan, light oxygenates, gases, and char. However, their model does not include several major products, such as acetic acid, furfural, formic acid, hydroxy acetone, anhydroxylose, dianhydroxylose, and other smaller molecules that have been experimentally measured in large yields.[34,35] Similarly, due to its complex chemical structure, lignin also requires the adoption of different reference components, as named by Faravelli et al.,[36] such as lignin rich in carbon (LIG-C), lignin rich in hydrogen (LIG-H), and lignin rich in oxygen (LIG-O). These reference components decompose releasing gases and intermediate components, which further degrade forming lighter species and lignin intermediate derivatives.[37]

Due to the elevated heat transfer coefficients through conduction and convection, biomass pyrolysis is most often carried out in fluidized bed reactors.[38] However, difficulties associated with the heat carrier solids ultimately lead to challenges in the separation of the heat carrier from the pyrolysis products.[16] A drop tube reactor (DTR) where the solid particles fed at the top develop high heat flux and can replace the fluidized bed.[39] Even though low residence time results in low heat transfer and requires finely ground particles to achieve complete conversion, DTR remains an attractive technology due to its simplicity of operation. Indeed, DTR is a continuous flow reactor where feedstock and carrier gas (usually nitrogen) are fed from the top. A feeding system is typically used to control the feed rate of the reacting solid and the mass flow of carrier gas. The incoming feeds are heated by the vertical reactor tube to the reaction temperature. Char and volatile products are collected at the lower end of the reactor tube followed by solid separation and vapours condensation.

From a process optimization perspective, the development of models for simulating biomass pyrolysis is becoming increasingly important, and understanding pyrolysis kinetics is critical for designing, optimizing, and scaling up industrial biomass conversion. To this

aim, limited modelling studies have been reported, particularly considering biomass pyrolysis in DTR.[40] Studies reported by Humbird et al.,[41] and Caudle et al.,[42] in the Aspen custom modeller, are among the recent ones.

Most of the available literature is devoted to the characterization of the decomposition of CELL with poor understanding on the key pyrolytic products from HCE decomposition such as 3-hydroxypropanal ($C_3H_6O_2$), Glyoxal, furfural and acetic acid, of which acetic acid and furfural were reported to be typical products.[43] Indeed, acetic acid is the main carboxylic acid component obtained from biomass pyrolysis, especially from HCE dissociation of *O*-acetyl group[33] at low temperature and can be considered as a representative component for carboxylic acids.

Furthermore, pyrolysis process and pyrolyzed product distributions are affected by the type of biomass and structure of biomass reference components.[44,45] For instance, CELL yields more liquid than gas, HCE produces more gas and less liquid, and lignin produces more char and less liquid,[46] and in the same way, the proportion of individual liquid and gas products vary.[47]

Understanding fast pyrolysis in DTR for scale-up is then reported to be a challenge, requiring careful examination of specific rate-determining steps and addressing the question of whether the heat transfer mechanism is efficient and whether the residence time of the two phases is sufficient. This needs to be reported along with the biomass properties and their sub-components.

For simulating pyrolysis process in Aspen Plus, two process blocks can be used: the continuous stirred reactor (RCSTR) and the plug flow reactor (RPLUG). Due to its perfect mixing assumption,[48] RCSTR is mainly used to mimic pyrolysis from fluidized bed reactors, while RPLUG is able to study different configuration parameters such as optimal length, height, and diameter of the pyrolyzer.[49] Since the selection of the appropriate Aspen Plus block has a significant impact on process development, in the present study biomass pyrolysis from DTR has been modelled in Aspen Plus software using a RPLUG. This is because the radius of the DTR reactor is much smaller than the length so the change in concentration and temperature of both the solid and the vapour phases in the radial direction is very small as compared to the axial direction. Eventually, this work is devoted to the realization of a numerical characterization of industrial processes based on biomass pyrolysis, which included a newly developed kinetic model. More specifically, this mechanism considers the recent improvements and updated kinetic schemes with additional components from Ranzi et al.[50] and revised reaction mechanisms from Humbird et al.,[41] and Caudle et al.[42]

For these reasons, to guarantee the completeness and robustness of a kinetic mechanism, the validation should be extended to different biomass types with ranges of CELL, HCE, and lignin to be able to catch the effects of their structure on products trends. To this aim, the present study incorporated kinetics of these components as products from HCE pyrolysis, and considered different biomass types (i.e., oak; high lignin, rice straw; high HCE and low lignin, beechwood; high CELL, and cassava stalk; low HCE) for mechanism validation in order to evaluate the accuracy of the kinetic mechanism and the effects of the components interaction on yield products.

2 | NUMERICAL METHODS

This work presents a detailed analysis of physical–chemical phenomena characterizing biomass pyrolysis, aiming at the realization and implementation in real systems of a kinetic mechanism. The operative conditions to be analyzed were selected based on a comparison of characteristic time of main phenomena involving biomass decomposition. More specifically, to evaluate the dynamic system in the pyrolysis reactor, the characteristic time for reaction and diffusion rates for the rate-determining reactions have been evaluated. The characteristic time for the overall reaction is intended as the inverse of the reaction rate ($1/r$), whereas the characteristic time for diffusion is assumed as the square of characteristic length divided by diffusion coefficient (L^2/D), in accordance with the literature.[51–53] Furthermore, the pyrolysis model was tested and cross-checked with experimental data reported in the literature for different feedstocks[39,54–56] over a range of reaction conditions. Additional information on the specific steps composing the implemented procedure is provided in the following sections.

2.1 | Reaction modelling

The kinetic mechanism assembled in this work follows the approach proposed by Di Blasi et al.[57] where a linear interlinkage reaction process between the three biomass building blocks has been assumed.[58,59] The pyrolysis mechanism combines the kinetics of single-step reactions available in the current literature.[6,36,41,42,60–62] The main pyrolysis reaction of biomass is represented by 20 independent first-order reactions accounting for the recently revised and updated kinetic parameters.

The present work considers the decomposition and primary pyrolysis reactions and, thus, involves two phases. The first phase is the virtual reaction step where the biomass is decomposed into three representative

biochemical building blocks (i.e., CELL, HCE, and lignin) followed by the second phase where the three building blocks decompose via various reactions forming different pyrolysis products: liquid, gas, and char. This is a devolatilization stage where a kinetic mechanism is applied to study the biomass pyrolysis reaction process. It is an interrelated model of the separate decomposition reactions of CELL, HCE, and lignin as stated by Miller and Bellan[63] and Di Blasi.[57]

2.2 | Computational study

The computational model produced in this work is tested using Aspen Plus to simulate the biomass pyrolysis process. Aspen Plus is a process-oriented software that facilitates the calculation of physical, chemical, and biological parameters.[64] Biomass was set as an unconventional component with the global simulation stream class set to be MIXCINC (i.e., comprising both conventional and non-conventional solids). In the Aspen Plus, the empirical correlations of coal enthalpy and density methods were used as described in the current literature[65] to calculate the enthalpy and density of the unconventional component. A decomposition reaction is implemented in Aspen Plus using an RYield-type reactor for converting biomass into conventional components (i.e., CELL, HCE, lignin, and ash). In the simulation, $(C_6H_{10}O_5)n$ and $(C_5H_8O_4)n$ represent CELL and HCE,[65,66] respectively, whereas LIG-C $(C_{15}H_4O_4)n$, LIG-H $(C_{22}H_{28}O_9)n$, and LIG-O $(C_{20}H_{22}O_{10})n$ represents lignin.[36] These polymeric components' properties are not readily available in any process modelling software because of the heterogeneity of components and diverse property variables. For any process model to estimate the yields and mimic the process accurately the fidelity of the property model for various biomass types and components must prove its accuracy. For estimating the energy balance in a pyrolysis reactor, the enthalpy of formation of all the component species involving in the reactions must be accurate. Efforts on estimating the thermophysical properties are explored by Wooley et al.[67] Gorensek et al.[68] has developed in detail a method that is adopted in the present study to incorporate missing parameters of conventional solids such as molecular weights, standards solid enthalpy of formation, heat capacity model coefficients, and solid density to set a conventional biomass-based data bank. The ideal gas heat capacity, ideal gas heat of formation, and critical properties were estimated from the Aly-Lee equation,[69] whereas vapour pressure is obtained based on Pitzer vapour pressure correlation fitted to the Aspen Plus PLXANT extended Antonie model.[70] Peng–Robinson's (PR) cubic

equation of state with Boston−Mathias (BM) alpha function[71] was selected as a thermodynamic property method since it can accurately predict thermodynamic properties of interest for this study due to its closer compression factor (0.307) to that of real hydrocarbons (0.27–0.29).[72,73] This method, represented in Aspen Plus[74] as the PR−BM method, is the most commonly used property method in gas processing, refining, petrochemicals, and biomass pyrolysis applications.[41,62,75] Aspen Plus performs material and energy balance based on the product distribution and the specified heat of reaction of the components involved.[76] Details of components and their representation in the pyrolysis model can be found in Table S1 of the supplementary material.

The RPLUG was chosen to simulate the pyrolysis process, the kinetic reaction scheme was implemented as a power-law type kinetic expression, and the reaction rate was calculated in Aspen Plus following the Arrhenius-like equation expressing the rate of reaction r as a function of the pre-exponential factor k, the absolute temperature T, the temperature exponent n, the
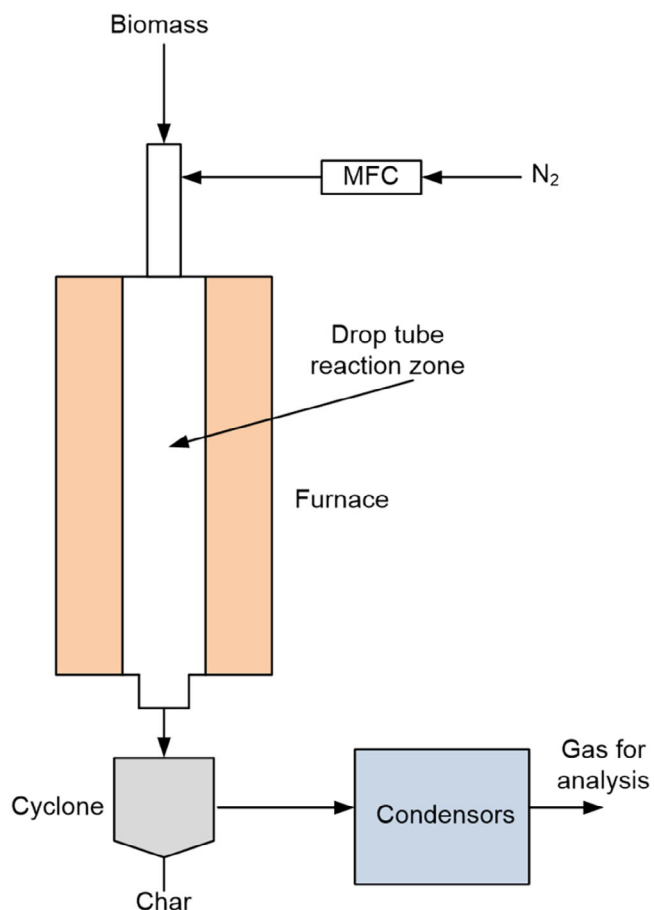

FIGURE 1 Schematic representation of biomass pyrolysis experimental set-up in drop tube reactor. MFC, mass flow controller.

activation energy Ea, and the gas law constant R as shown below in Equation (1).

$$r = k * T^n * \frac{e^{-Ea}}{RT} \qquad (1)$$

The chemical components and their representations used in the present study can be found in Table S1 of the supplementary material. Experimental conditions and assumptions reported in the literature[39,54–56] were numerically mimicked in Aspen Plus as shown in Figure 1. The operational conditions considered for fast pyrolysis simulation include the following: temperature 450–550°C, gas flow rate 1 L/min, biomass particle size 370 μm, reactor length 2 m, and reactor diameter 0.025 m. The temperature range chosen for analysis was considered as the temperature range that gave maximum liquid yield and fast quenching of the pyrolyzed vapours

TABLE 1 Feedstock compositions and conditions used for the simulation.[39,54–56]

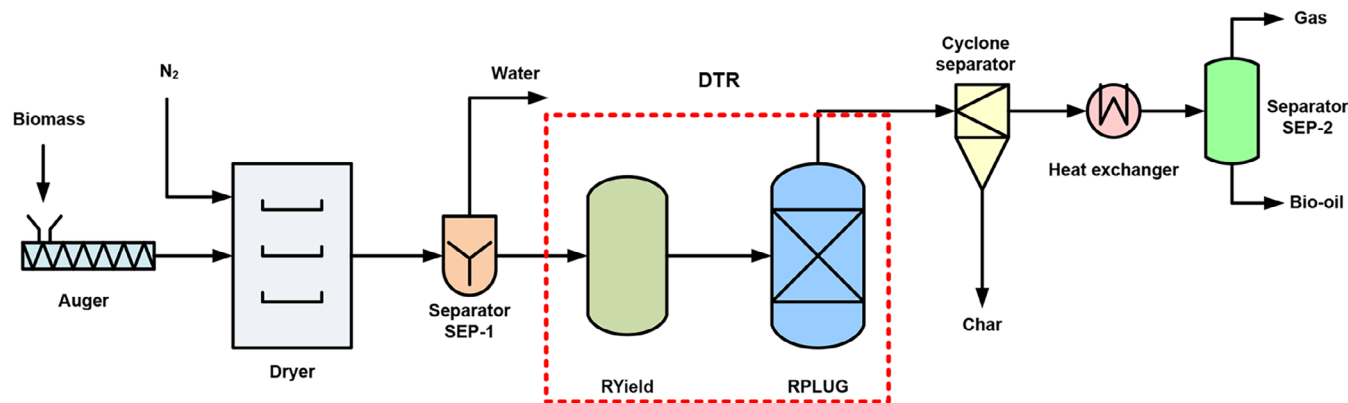| Biomasses				
Composition	**Oak (wt.%)**	**Beechwood (wt.%)**	**Rice straw (wt.%)**	**Cassava stalk (wt.%)**
Cellulose	29.8	40.26	35	47
Hemicellulose	20.0	21.68	36	14
Lignin	43.3	19.91	12.3	30.18
Ash	0.4	0.5	19.5	7.1
Extractives	3.3	14.07	14.17	5.69
Others	3.2	3.58	2.3	-
Proximate analysis				
Moisture	3.9	8.7[ar]	10.8	8.5
Volatiles	81.9	84.3[db]	66.89	69.7
Fixed carbon	12.6	15.2[db]	14.57	14.7
Ash	0.4	0.5[db]	19.5	7.1
Others	1.2	-	-	-
Ultimate analysis				
Carbon	48.7	49.1	39.98	48.8
Hydrogen	6.8	5.7	2.45	6.7
Oxygen	44	44.5	52.61	43.4
Nitrogen	<0.1	0.15	4.43	1.1
Sulphur	<0.1	0.045	0.53	0.0
Ash	0.4	0.5	19.5	7.1

Abbreviations: ar, as received; db, dry basis.

FIGURE 2 Schematic process model adopted for fast pyrolysis in a drop tube reactor. DTR, drop tube reactor.

during fast pyrolysis, which is 450–550°C.[77] To represent the wide variety of biomass fast pyrolysis, Oak, beechwood, rice straw, and cassava stalk were selected for validation because of the variations in the fraction of the chemical components that they have (i.e., high ligin, high CELL, low lignin, and low HCE, respectively), which ultimately dictate the product composition and yields. The detailed composition of the feedstocks is shown in Table 1. The DTR experimental set-up shown in Figure 1 was numerically represented in Aspen Plus as shown in Figure 2.

3 | RESULTS AND DISCUSSION

The set of 20 reactions representing the fast pyrolysis is shown in Table 2. The kinetic mechanism produced

TABLE 2 Selected reactions representative of biomass pyrolysis and the corresponding kinetic parameters available in the current literature.[6,50] Component names are taken from Gorensek et al.[68] Units, T (K).

#	Pyrolysis reactions	A (s^{-1})	n	Ea/T
	Cellulose			
1	CELL → CELLA	4.10^{13}	0	22,647.2
2	CELLA → 0.8 HAA + 0.2 GLYOX + 0.1 CH_3CHO + 0.25 HMFU + 0.3 C_3H_6O + 0.21 CO_2 + 0.1 H_2 + 0.4 CH_2O + 0.16 CO + 0.83 H_2O + 0.02 HCOOH + 0.61 Char	5.10^8	0	14,594.8
3	CELLA → LVG	$1.8.10^0$	1	5032.7
4	CELL → 5 H_2O + 6 Char	4.10^7	1	19,627.6
	Hemicellulose			
5	HCE → 0.4 HCE1 + 0.6 HCE2	$3.3.10^9$	0	15,601.4
6	HCE1 → 0.025 H_2O + 0.775 CO_2 + 0.025 HCOOH + 0.5 CO + 0.8 CH_2O + 0.125 C_2H_5OH + 0.55 CH_3OH + 0.25 C_2H_4 + 0.125 H_2 + 0.4 COH_2 + 0.325 CH_4 + 0.875 Char	1.10^9	0	16,104.7
7	HCE1 → 0.25 H_2O + 0.75 CO_2 + 0.05 HCOOH + 0.45 CO + 0.375 C_2H_4 + 1.7 COH_2 + 0.625 CH_4 + 0.675 Char	5.10^{-02}	1	4026.2
8	HCE1 → 0.6 XYLAN + 0.2 $C_3H_6O_2$ + 0.12 GLYOX + 0.2 FURF + 0.4 H_2O + 0.08 H_2 + 0.16 CO	3.10^0	1	5536.0
9	HCE2 → 0.2 H_2O + CO + 0.575 CO_2 + 0.4 CH_2O + 0.1 C_2H_5OH + 0.05 HAA + 0.35 ACAC + 0.025 HCOOH + 0.25 CH_4 + 0.3 CH_3OH + 0.225 C_2H_4 + 0.725 H_2 + Char	$5.0.10^9$	0	15,853.0
	Lignin			
10	LIGC → 0.35 LIGCC + 0.1 COUMARYL + 0.08 PHENOL + 0.41 C_2H_4 + H_2O + 0.3 CH_2O + 0.32 CO + 0.7 COH_2 + 0.495 CH_4 + 5.735 Char	$1.33.10^1$	0	24,408.7
11	LIGH → LIGOH + C_3H_6O	$6.7.10^{12}$		18,872.7
12	LIGO → LIGOH + CO_2	$3.3.10^8$	0	12,833.4
13	LIGCC → 0.3 COUMARYL + 0.2 PHENOL + 0.35 HAA + 0.7 H_2O + 0.6 C_2H_4 + 0.8 CO + COH_2 + 0.65 CH_4 + 6.75 Char	$1.6.10^6$	0	15,853.0
14	LIGOH → LIG + 0.15 H_2 + 0.9 H_2O + 0.45 CH_4 + CH_3OH + 0.05 CO_2 + 1.3 CO + 0.05 HCOOH + 0.2 C_2H_4 + 0.6 COH_2 + 4.15 Char	5.10^7	0	15,098.1
15	LIGOH → 1.5 H_2O + 2.1 CO + 1.75 CH_4 + CH_3OH + 0.5 H2 + 3.9 COH_2 + 0.3 C_2H_4 + 0.5 CH_3OH + 10.15 Char	$3.3.10^1$	0	7549.07
16	LIG → 0.7 FE2MARC + 0.3 ANISOLE + 0.6 CO + 0.3 CH_3CHO	4.10^0	1	6039.3
17	LIG → 0.95 H_2O + 0.2 CH_2O + 0.4 CH_3OH + 1.45 CO + 0.6 CH_4 + 0.05 HCOOH + 0.5 COH_2 + 0.65 C_2H_4 + 0.2 CH_3CHO + 0.2 C_3H_6O + 5.5 Char	4.10^8	0	15,098.1
18	LIG → 0.6 H_2O + 0.6 CO + 0.6 CH_4 + 0.4 CH_2O + 0.5 C_2H_4 + 0.4 CH_3OH + 2 COH_2 + 6 Char	$8.3.10^{-02}$	1	4026.2
	Water			
19	$H_2O(L)$ → $H_2O(V)$	$5.13.10^6$	0	10,583.8
	Metaplastic			
20	COH_2 → CO + H_2	5.10^{11}	0	35,732.3

Abbreviations: ACAC, acetic acid; CELL, cellulose; CELLA, activated cellulose; FURF, furfural; HAA, hydroxy acetaldehyde; HCE1, hemicellulose intermediate 1; HCE2, hemicellulose intermediate 2; HMFU, hydroxymethyl furfural; LIGC, Lignin rich in carbon; LIGCC, Lignin intermediate rich in carbon; LIGH, Lignin rich in hydrogen; LIGOH, Lignin intermediate rich in oxygen and hydrogen.

in this work can be intended as the sum of three sub-mechanisms, accounting for CELL (CELL), HCE, and lignin (LIGN) decomposition.

Figure 3A–C depicts the comparison of rate constants of reactions considered in the current kinetic mechanism (as reported in Table 2) versus inverse of pyrolysis temperature. In order to identify the slowest step of the chemical reaction that determines the rate at which the overall pyrolysis reaction proceeds, the rate constant of each reaction responsible for the decomposition of CELL, HCE, and lignin have been evaluated as a function of the inverse of pyrolysis temperature. As can be seen from the figures, it is quite clear that regardless of the pyrolysis temperature, reactions 3, 7, and 18, respectively, are found to be the rate determining steps (i.e., slowest) during CELL, HCE, and lignin pyrolysis.

Once the rate-determining step during the decomposition of each reference component is identified, diffusion and reaction characteristic times are determined, as shown in Figure 3. From the plot, it is clear that the characteristic time for the diffusion is much smaller than the chemical characteristic time for any investigated conditions. This trend indicates that the pyrolysis process is the rate-determining step, and thus the selected conditions can be used for a representative analysis of kinetic parameters (Figure 4).

The effect of pyrolysis temperatures on the yield of pyrolysis products (i.e., bio-oil, gas, and char) is analyzed and shown in Figure 5–7. The pattern of the pyrolysis yield change with the reaction temperature (i.e., 450, 500, 550°C) has been evaluated and discussed.

Figure 5A oak shows that the yield of bio-oil shows an almost constant trend with the rise in temperature from 450 to 550°C. Similarly, in Figure 5B beechwood—the yield of bio-oil increased from 49 to 64 wt.% as temperature increased from 450 to 500°C. Further increasing the temperature to 550°C decreases the yield of bio-oil. Likewise, in Figure 5C rice straw and Figure 5D cassava stalk—the yield of the bio-oil increases with an increase of the temperature from 450 to 500°C, and showed a decreasing trend when the temperature was increased further. In all cases, the decrease in bio-oil yield with an
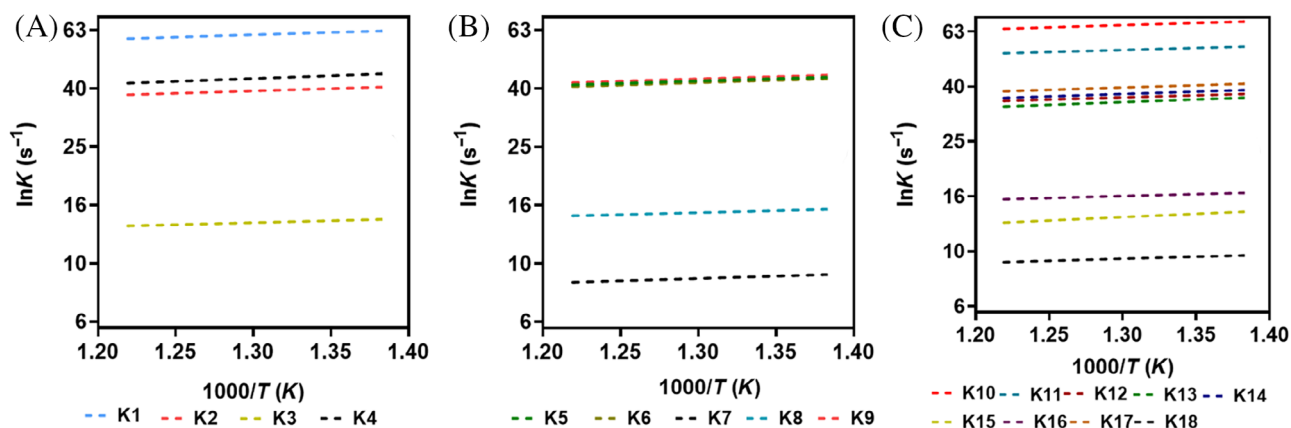

FIGURE 3 Rate constant versus inverse of temperature for (A) cellulose, (B) hemicellulose, and (C) lignin.
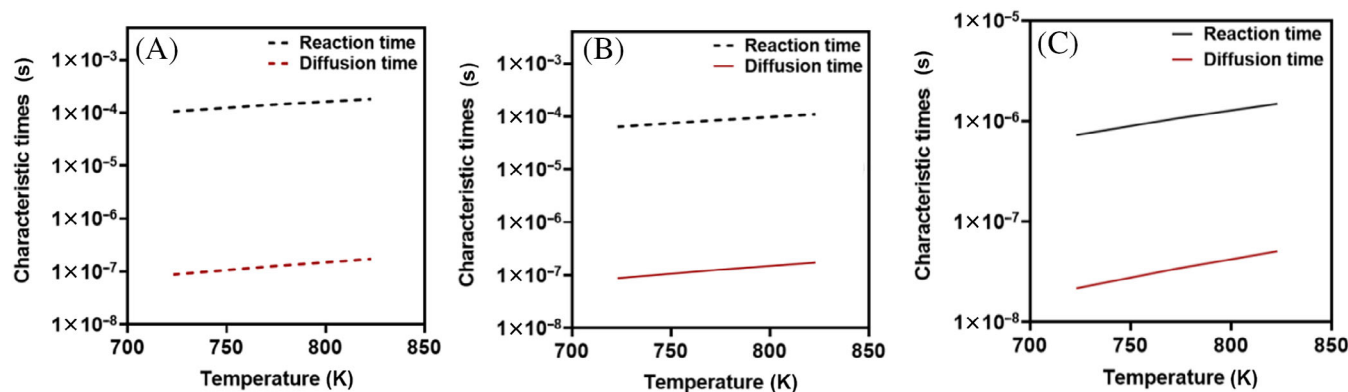

FIGURE 4 Reaction rate and diffusion characteristic times at different pyrolysis temperatures: (A) hemicellulose, (B) lignin, (C) cellulose.
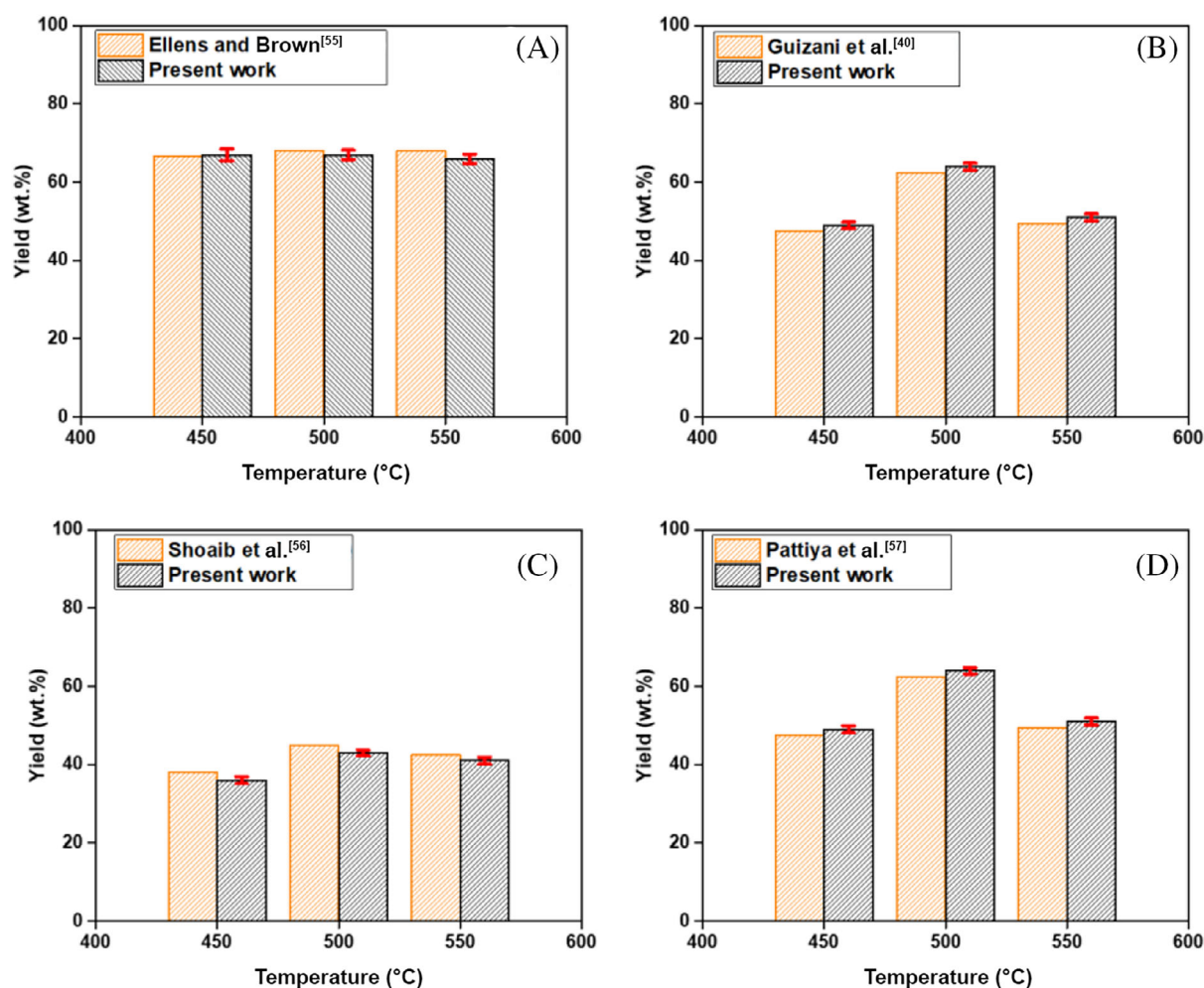
FIGURE 5 Bio-oil product distribution from different feedstocks: (A) oak, (B) beechwood, (C) rice straw, and (D) cassava stalk. Green graph bars represent experimental results from Ellens and Brown, Guizani et al., Shoaib et al., and Pattiya et al.,[39,54–56] respectively. Black graph bars are simulation results from the present work.

increase in temperature is due to the secondary reactions favouring the yield of gas over liquid product. The difference in bio-oil yield for the different feedstocks can be explained by the difference in the fraction of CELL, HCE, and lignin in the feed. Overall, for the investigated biomasses, further increasing of temperature to 550°C did not favour the yield of liquid components, and thus, the optimum pyrolysis temperature is found to be 500°C.

On the other hand, the yield of gas is shown in Figure 6A–D. For all investigated feedstocks, the yield of gas increased with an increase in temperature, which is due to the initiation of secondary reactions at higher temperatures, which favours the formation of gas components. In the same way, the difference in gas yield for all feedstocks is due to the difference in the fraction of CELL, HCE, and lignin in the initial biomass feed. Comparably, rice straw and cassava stalk are found to have a high yield of gas than oak and beechwood, which could

be due to the higher ash content in the feedstock. The same conclusion has been drawn by Trendewicz et al.[78]

Furthermore, the yield of char from the pyrolysis of oak, beechwood, rice straw, and cassava stalk pyrolysis has been shown in Figure 7A–D. As can be seen from the figure, the yield of char decreased with increasing pyrolysis temperature, which is associated with the increase in the reactivity of the reacting components favouring the production of liquid and gas products. The relatively high yield of char observed from rice straw could be related to the high ash content in feed. Overall, the present study is in fair agreement with the pyrolysis yields of experimental results reported in literature.[39,54–56]

To better understand the influence of reaction conditions and feedstock compositions on individual gas compositions, the yield of CO_2, CO, H_2, CH_4, and C_2H_4 from oak, beechwood, rice straw, and cassava stalk has been numerically evaluated and plotted in Figure 8A–D. Clearly, due to the high fraction of CELL and HCE,
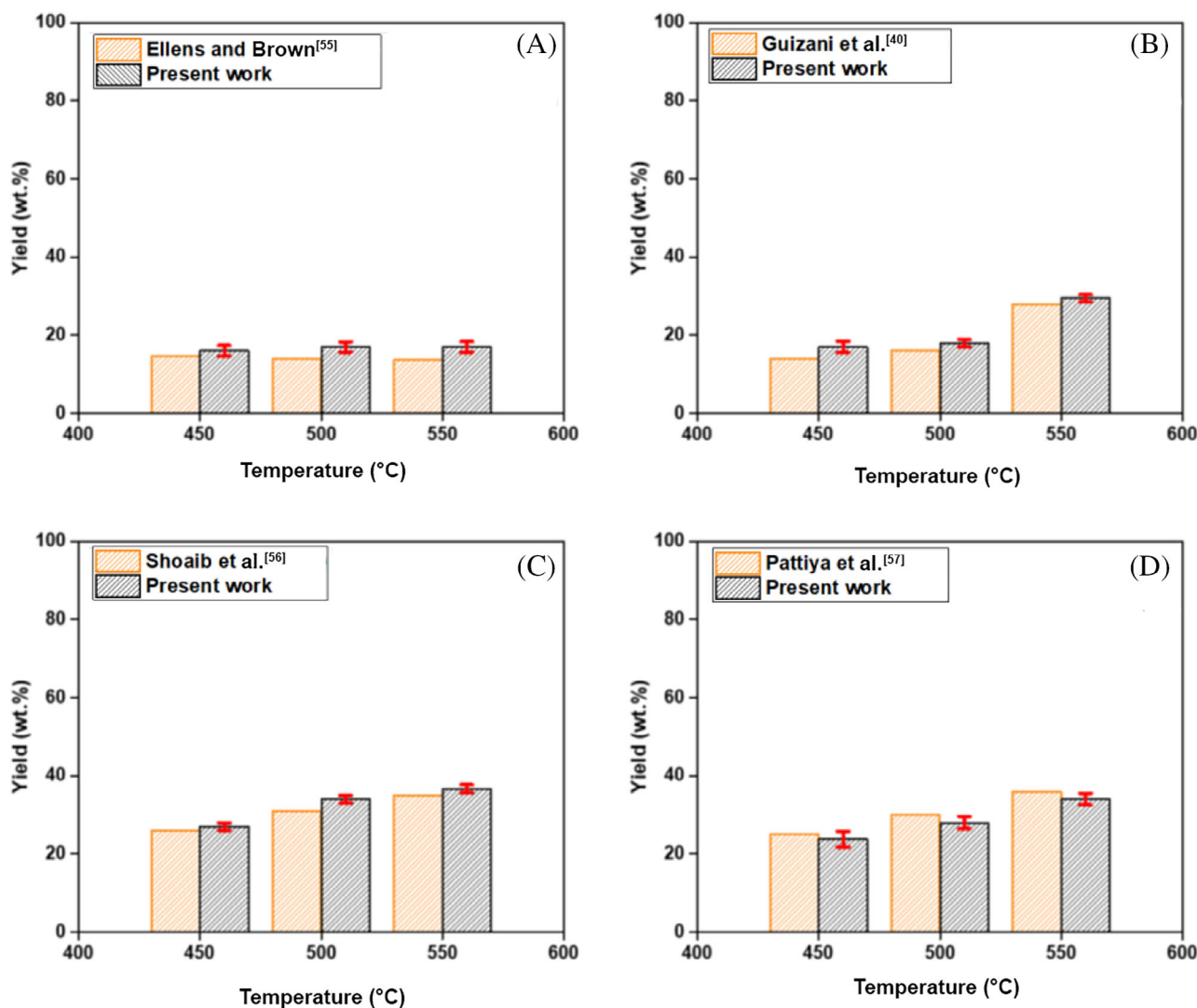
FIGURE 6 Gas yield distribution from different feedstocks: (A) oak, (B) beechwood, (C) rice straw, and (D) cassava stalk. Green graph bars represent experimental results from Ellens and Brown, Guizani et al., Shoaib et al., and Pattiya et al.,[39,54–56] respectively. Black graph bars are simulation results from the present work.

a relatively high yield of gas composition has been observed in cassava, beechwood, and rice straw, whereas oak yields quite low gas, compared to the others. The reason for this could be due to the high CELL and HCE fractions in rice straw, which led to high hydrogen fraction. Under the studied condition, despite the magnitude of the increment, the yield of all gases increased with increasing temperature. For instance, the increase in CO concentration can be associated with the decomposition of CELL due to the thermal cracking of carboxyl (C=O) and carbonyl (C—O—C)[79] and with the initiation of secondary reactions.[80] Similarly, the high fraction of CO_2 can be related to the degradation of HCE, which is a major contributor to CO_2, owing to the high content of carboxyl groups.[81] These results are in agreement with the works of Lai and colleagues.[82] The lower yields of

H_2 and CH_4 are mainly due to the wide degradation temperature behaviour of lignin, which is the main contributor of H_2 and CH_4 due to the presence of methoxyl—O—CH_3 and aromatic rings with several branches.[79] From the analysis, it can be mentioned that higher temperature favours the yield of hydrogen gas for all feedstocks, with a high fraction for rice straw, and a lower fraction in oak (i.e., rice straw > beechwood > cassava stalk > oak). Besides, it can also be noted that higher pyrolysis temperature can favour the fraction of syngas, and thus, higher and lower yields are observed in cassava and oak, respectively, which could be due to the large difference in CELL composition.

Furthermore, the yield of individual gas components obtained in this study has been compared with the gas chromatography mass spectroscopy (GC–MS) results available in the current literatures.[39,83,84] It can be
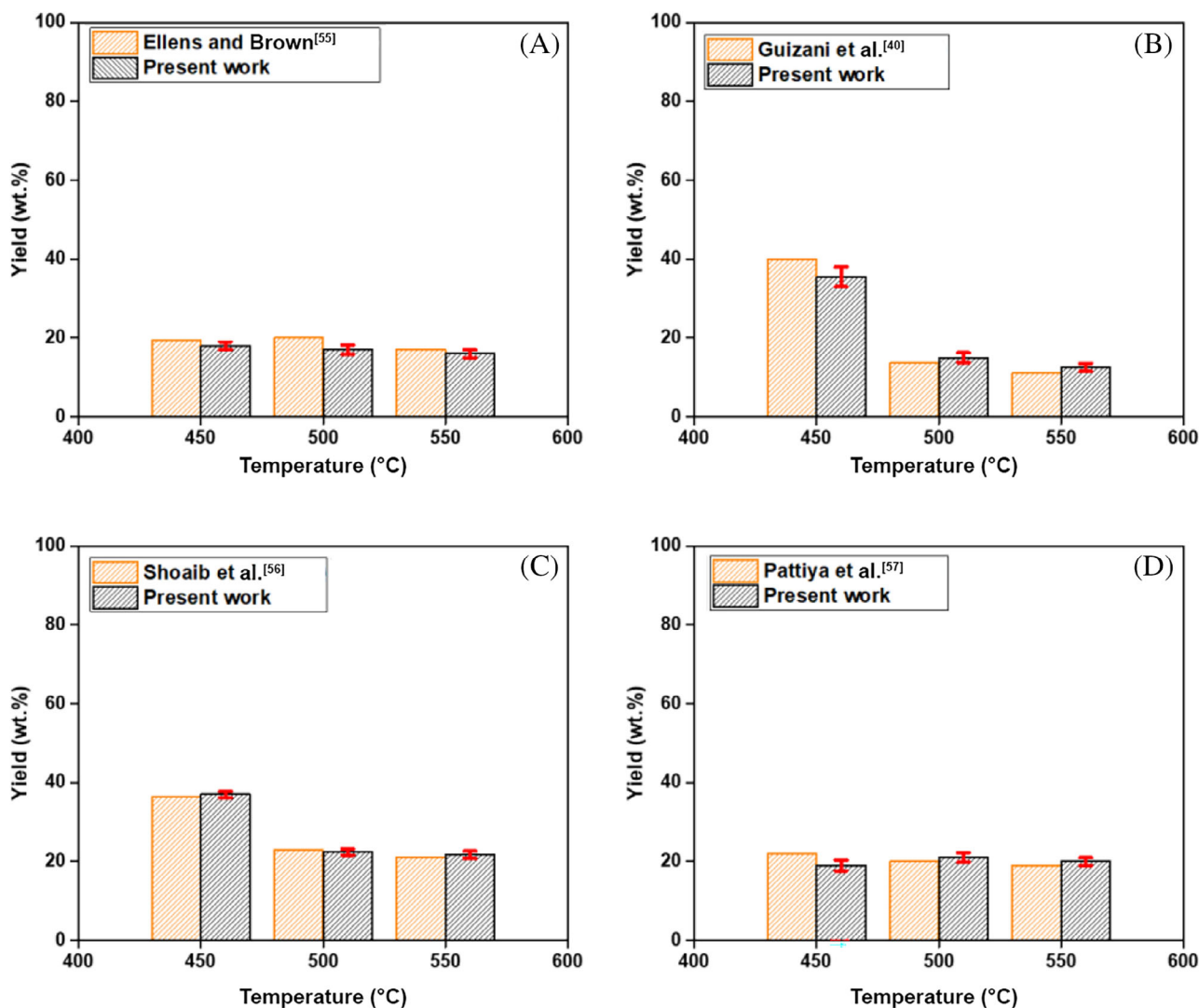
FIGURE 7 Char yield from different feedstocks: (A) oak, (B) beechwood, (C) rice straw, and (D) cassava stalk. Green graph bars represent experimental results from Ellens and Brown, Guizani et al., Shoaib et al., and Pattiya et al.,[39,54–56] respectively. Black graph bars are simulation results from the present work.

concluded from the table that the current simulation results agree with experimental results with not more than 12% variation (for CO_2) (Table 3).

In addition to yields, the composition of the bio-oil is also important as it determines the stability and quality of the bio-oil and its suitability for upgrading. With this in mind, to better visualize the effect of pyrolysis temperature on the fractions of the basic bio-oil chemical families, the yields of different bio-oil components were analyzed and shown in Figure 9.

Figure 9A–D depicts the detailed bio-oil compositions broken down into basic bio-oil constituents as obtained from the simulation (detailed composition by functional groups) from oak, beechwood, rice straw, and cassava stalk pyrolysis, respectively. As can be seen from the figure, different species of the bio-oil chemical family

showed different trends in the pyrolysis temperature. For instance, the yield of aldehyde increases sharply with increasing pyrolysis temperature. The rise in pyrolysis temperature from 450 to 500°C, increases the yield of aldehydes by 8%. A further increase of the temperature to 550°C surges the aldehydes content by another 6%, reaching a total increment of 14%. This is due to the initiation of secondary reactions of the intermediate components (particularly the sugar derivatives) with the rising temperature. The increasing trend of aldehydes yield with an increase in pyrolysis temperature is consistent with the study reported by Fernandez et al.,[85] on pinewood.

On the contrary, anhydrosugar derivatives sharply decrease with an increase in pyrolysis temperature, thus indicating quick degradation of the component at higher temperatures. For example, the first increase in
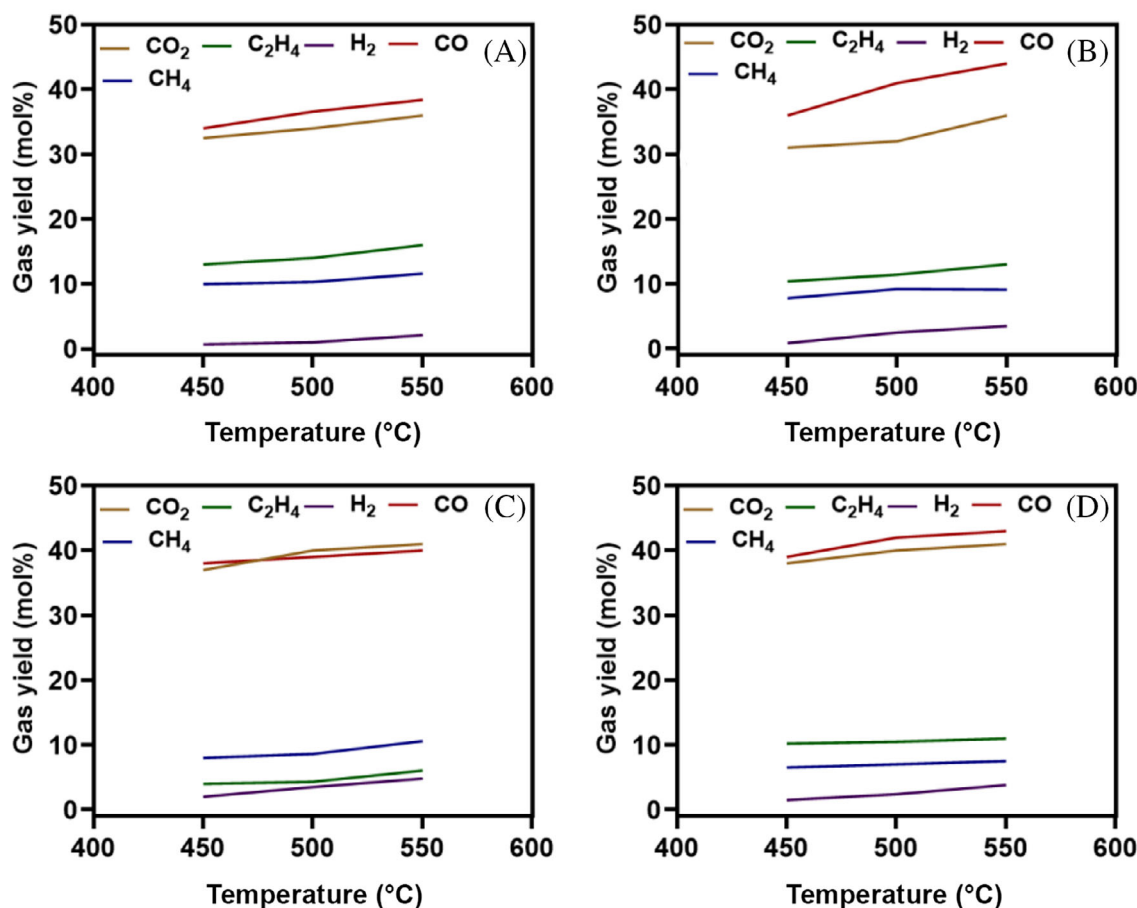
FIGURE 8 Effect of pyrolysis temperature on the individual composition of gases produced from fast pyrolysis of (A) oak, (B) beechwood, (C) rice straw, and (D) cassava stalk.

TABLE 3 Yield of non-condensable gases obtained from pyrolysis of oak, beechwood, and rice straw at 500°C.

Gas (mol%)	Oak		Beechwood		Rice straw	
	Sim.	Lit.[83]	Sim.	Lit.[39]	Sim.	Lit.[84]
CO_2	34	47.7	32	22	39	50
CO	37	38.8	41	58	38	33.6
H_2	1.0	1.3	2.5	3.8	3.5	4.2
CH_4	10.3	10.5	9.2	10.4	8.6	9.0
C_2H_4	14	-	10.4	3.0	4.3	3.33

temperature from 450 to 500°C results in a decrease in sugar derivatives yields by 10% in the case of oak and beechwood and by 13%–16% for rice straw and cassava stalk. When the pyrolysis temperature further rises to 550°C, the yield of anhydrosugar in the bio-oil halted by around 10%. Overall, the further degradation of the sugar derivatives triggered by increasing pyrolysis temperature indicates the enhancement of LVG degradation through a ring-opening reaction of glycosidic1,6-acetal bond forming HAA. From this, it can be noted that LVG can

also act as an intermediate component for the formation of other lighter products in CELL pyrolysis. The results are consistent with studies reported by several authors.[20,86–88] A higher fraction of anhydrosugar, which is one of the main contributors to the bio-oil acidity, is observed in bio-oil obtained from rice straw and beechwood pyrolysis followed by cassava stalk and the least in oak, possibly due to higher CELL and HCE composition in rice straw, beechwood, and cassava, respectively.

Finally, the rise in temperature from 450 to 500°C favoured the yield of alcohols by 2%. However, further increasing the temperature to 550°C did not show a significant effect on the yield. In the same way, the change in the temperatures resulted in an increase in ketones yield by around 2%. The variation in the fraction of acids and phenols happens to be insignificant with the change in the pyrolysis temperature. This indicates lower sensitivity of bio-oil acidity towards pyrolysis temperatures. Comparatively, high and low acid fractions have been observed in rice straw and cassava stalk, respectively, which is due to high HCE content in rice straw and low HCE composition in cassava stalk feedstock. Similarly,
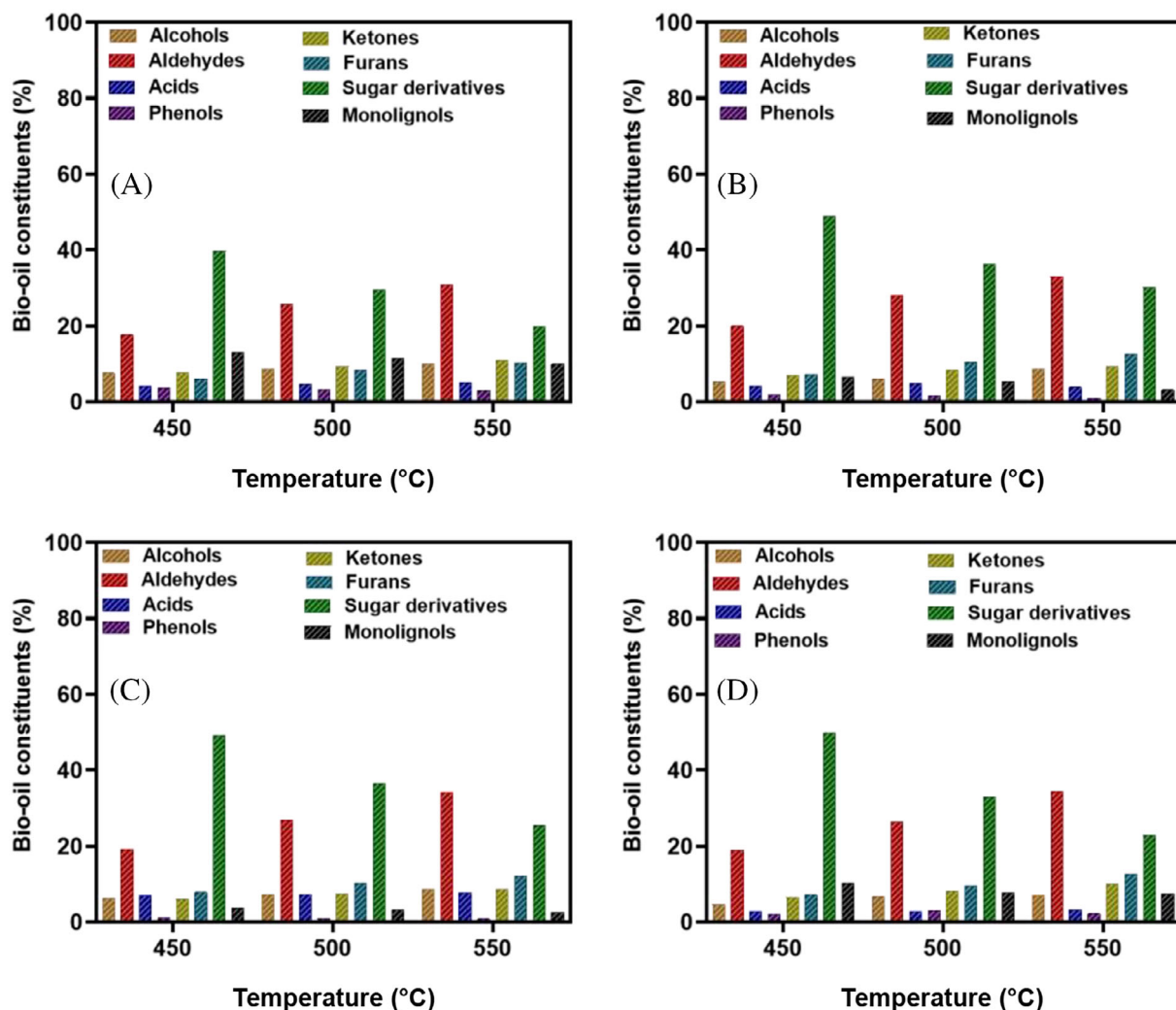
FIGURE 9 Bio-oil constituent distribution at different pyrolysis temperatures: (A) oak, (B) beechwood, (C) rice straw, and (D) cassava stalk.

the high yield of phenols in oak and the low yield of phenols in rice straw can be associated with the lignin composition in the feedstocks. In contrast, the yield of furans was found to be slightly increased with an increase in temperature, which is due to further conversion of xylose to furfural, whereas the share of monolignols such as coumaryl alcohol and sinapyl aldehyde was found to show a decreasing trend with the increasing temperature, indicating the further decomposition of the lignin intermediates to lighter components.

The distribution of light oxygenates, aromatics, and anhydrous sugars in the bio-oil composition has been compared in Figure 10. The yield of light oxygenates such as hydroxy acetone, acetone, HAA, glyoxal, acetaldehyde, acetic acid, ethanol, methanol, formic acid, and formaldehyde increased with increasing the pyrolysis temperature and were apparently due to the secondary reaction

of anhydrous sugars, aromatic compounds, and/or their intermediates as described in the literature.[89,90] The yield of light oxygenates increased from 33% at 450°C to 59% at 550°C, in agreement with the study reported in the literature.[91] The trend of anhydrosugar with the pyrolysis temperature has been discussed above. On the other hand, the yield of aromatic components did not show an obvious change when the temperature increased from 450 to 550°C. The low yield of the aromatic compound in the case of rice straw is due to the low lignin component in the feed. In general, the increase in pyrolysis temperature resulted in a decrease in anhydrous sugar and eventually an increase in light oxygenates fraction, but which did not significantly impact the yield of aromatic components. The trends of bio-oil components, especially anhydrous sugar and light oxygenates, remain consistent with the study reported in the literature.[92]

FIGURE 10 The share of light oxygenates, aromatic compounds and anhydrosugars in the bio-oil obtained from (A) oak, (B) beechwood, (C) rice straw, and (D) cassava stalk pyrolysis.
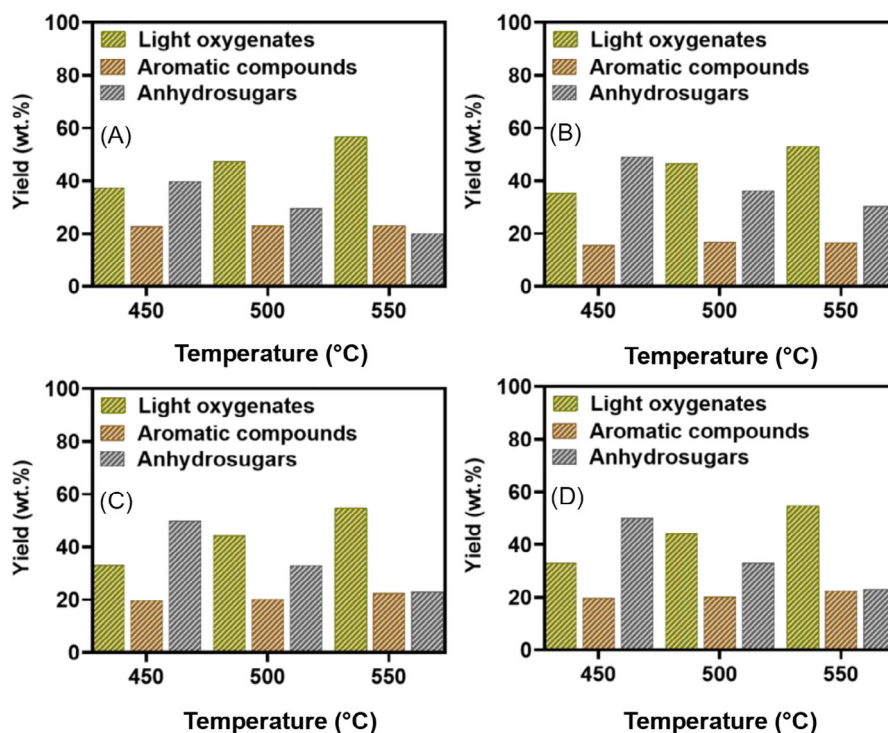
4 | CONCLUSIONS

Biomass pyrolysis from a DTR was modelled as a plug flow reactor using Aspen Plus simulation software and a detailed kinetic mechanism for heterogeneous reactions. Main phenomena governing biomass pyrolysis process were analyzed, observing that pyrolysis is controlled by the chemistry of the system than diffusion rate. The pyrolysis process and the product distributions throughout pyrolysis temperatures (i.e., 450, 500, and 550°C) were studied. The effect of pyrolysis temperature on the yield of liquid, solid, and gas products was evaluated. Due to the structural difference in CELL, HCE, and lignin, the difference in feedstock composition was found to play role in pyrolyzed product distributions. Oak and beechwood biomasses were found to give high yield of bio-oil while rice straw was found to yield higher gas and char than other biomasses. In addition, the variation of individual bio-oil components with pyrolysis temperature was analyzed. Under the studied conditions, an optimum yield of bio-oil was obtained at 500°C for all feedstocks except for cassava stalk, where maximum bio-oil was obtained at 450°C. Besides, in all feedstocks, the share of light oxygenates outweighs the fraction of anhydrous sugar and aromatic compounds. Overall, the kinetic mechanism and the pyrolysis process model are in good agreement with the experimental data, demonstrating the validity of the developed model as a predictive tool for biomass pyrolysis. The ability of the model to capture product trends from different biomass types is a good indicator that the model can potentially be used for biomass processing. However, taking into account further decomposition kinetics of main intermediates would help to understand the effect of possible interactions among each particle on product composition. Therefore, the authors recommend the future work should consider further decomposition of larger molecular weight intermediates, which would help to improve the yield of desired fractions and reduce the oxygen functionality of the components apparently improving the heating value, which is one of the challenges in pyrolysis scale-up.

NOMENCLATURE

DTR	drop tube reactor
HAA	hydroxy acetaldehyde
LVG	levoglucosan
RPLUG	plug flow reactor
CELL	cellulose
CELLA	activated cellulose
HCE	hemicellulose
HCE1	hemicellulose intermediate 1
HCE2	hemicellulose intermediate 2
LIG-O	lignin rich in oxygen
LIG-H	lignin rich in hydrogen

LIG-C   lignin rich in carbon
LIGOH   lignin intermediate rich in oxygen and hydrogen
LIGCC   lignin intermediate rich in carbon

AUTHOR CONTRIBUTIONS

Fekadu Mosisa Wako: Data curation; formal analysis; investigation; methodology; software; validation; visualization; writing – original draft; writing – review and editing. **Gianmaria Pio:** Conceptualization; supervision; visualization; writing – review and editing. **Ashraf Lofti:** Resources; software; visualization; writing – review and editing. **Ernesto Salzano:** Conceptualization; resources; supervision; writing – review and editing. **Azharuddin Farooqui:** Software; visualization; writing – review and editing. **Nader Mahinpey:** Conceptualization; resources; supervision; writing – review and editing.

PEER REVIEW

The peer review history for this article is available at https://www.webofscience.com/api/gateway/wos/peer-review/10.1002/cjce.24964.

DATA AVAILABILITY STATEMENT

The authors confirm that all data supporting the findings of this study are included in the article.

ORCID

Fekadu Mosisa Wako https://orcid.org/0000-0003-3928-0612
Gianmaria Pio https://orcid.org/0000-0002-0770-1710
Ernesto Salzano https://orcid.org/0000-0002-3238-2491
Nader Mahinpey https://orcid.org/0000-0001-8477-7228

REFERENCES

[1] X. Hu, M. Gholizadeh, *J. Energy Chem.* **2019**, *39*, 109.
[2] C. Mandil, *World Energy Outlook 2004*, International Energy Agency (IEA), Paris **2004**.
[3] E. Ranzi, M. Corbetta, F. Manenti, S. Pierucci, *Chem. Eng. Sci.* **2014**, *110*, 2.
[4] A. V. Bridgwater, D. Meier, D. Radlein, *Org. Geochem.* **1999**, *30*, 1479.
[5] A. Bridgwater, *J. Anal. Appl. Pyrolysis* **1999**, *51*, 3.
[6] E. Ranzi, A. Cuoci, T. Faravelli, A. Frassoldati, G. Migliavacca, S. Pierucci, S. Sommariva, *Energy Fuels* **2008**, *22*, 4292.
[7] M. S. Mettler, D. G. Vlachos, P. J. Dauenhauer, *Energy Environ. Sci.* **2012**, *5*, 7797.
[8] P. E. A. Debiagi, C. Pecchi, G. Gentile, A. Frassoldati, A. Cuoci, T. Faravelli, E. Ranzi, *Energy Fuels* **2015**, *29*, 6544.
[9] C. Koufopanos, A. Lucchesi, G. Maschio, *Can. J. Chem. Eng.* **1989**, *7*, 67.
[10] G. Varhegyi, M. J. Antal Jr.., E. Jakab, P. Szabó, *J. Anal. Appl. Pyrolysis* **1997**, *42*, 73.
[11] T. Faravelli, A. Frassoldati, E. Barker Hemings, E. Ranzi, in *Cleaner Combustion: Developing Detailed Chemical Kinetic Models* (Eds: F. Battin-Leclerc, J. M. Simmie, E. Blurock), Springer Science & Business Media, Berlin **2013**, p. 111.
[12] R. Vinu, L. J. Broadbelt, *Annu. Rev. Chem. Biomol. Eng.* **2012**, *3*, 29.
[13] A. Anca-Couce, *Prog. Energy Combust. Sci.* **2016**, *53*, 41.
[14] M. B. Pecha, J. I. M. Arbelaez, M. Garcia-Perez, F. Chejne, P. N. Ciesielski, *Green Chem.* **2019**, *21*, 2868.
[15] C. Di Blasi, *Prog. Energy Combust. Sci.* **1993**, *19*, 71.
[16] A. V. Bridgwater, *Biomass Bioenergy* **2012**, *38*, 68.
[17] S. Hameed, A. Sharma, V. Pareek, H. Wu, Y. Yu, *Biomass Bioenergy* **2019**, *123*, 104.
[18] F. Shafizadeh, A. G. W. Bradbury, *J. Appl. Polym. Sci.* **1979**, *23*, 1431.
[19] F. Shafizadeh, *J. Appl. Polym. Sci.* **1982**, *3*, 283.
[20] J. Piskorz, D. Radlein, D. S. Scott, *J. Appl. Polym. Sci.* **1986**, *9*, 127.
[21] J. Piskorz, D. S. A. Radlein, D. S. Scott, S. Czernik, in *Research in Thermochemical Biomass Conversion* (Eds: A. V. Bridgwater, J. L. Kuester), Elsevier Applied Science, London **1988**, pp. 557–571.
[22] G. N. Richards, *J. Anal. Appl. Pyrolysis* **1987**, *10*, 251.
[23] A. D. Pouwels, G. B. Eijkel, J. J. Boon, *J. Anal. Appl. Pyrolysis* **1989**, *14*, 237.
[24] J. Lomax, J. Commandeur, P. Arisz, J. Boon, *J. Anal. Appl. Pyrolysis* **1991**, *19*, 65.
[25] J. Piskorz, D. S. A. Radlein, D. S. Scott, S. Czernik, *J. Anal. Appl. Pyrolysis* **1989**, *16*, 127.
[26] J. L. Banyasz, S. Li, J. L. Lyons-Hart, K. H. Shafer, *J. Anal. Appl. Pyrolysis* **2001**, *57*, 223.
[27] J. Banyasz, S. Li, J. Lyons-Hart, K. Shafer, *Fuel* **2001**, *80*, 1757.
[28] Z. Luo, S. Wang, Y. Liao, K. Cen, *Ind. Eng. Chem. Res.* **2004**, *43*, 5605.
[29] X. Zhou, W. Li, R. Mabon, L. J. Broadbelt, *Energy Technol.* **2017**, *5*, 217.
[30] P. Giudicianni, V. Gargiulo, M. Alfè, R. Ragucci, A. I. Ferreiro, M. Rabacal, M. Costa, *J. Anal. Appl. Pyrolysis* **2019**, *137*, 266.
[31] V. Gargiulo, P. Giudicianni, M. Alfe, R. Ragucci, *Journal of Chemistry* **2019**, *2019*, 1.
[32] V. Gargiulo, A. I. Ferreiro, P. Giudicianni, S. Tomaselli, M. Costa, R. Ragucci, M. Alfe, *J. Anal. Appl. Pyrolysis* **2022**, *161*, 105369.
[33] D. Shen, S. Gu, A. V. Bridgwater, *J. Anal. Appl. Pyrolysis* **2010**, *87*, 199.
[34] X. Zhou, W. Li, R. Mabon, L. J. Broadbelt, *Energy Environ. Sci.* **2018**, *11*, 1240.
[35] P. R. Patwardhan, R. C. Brown, B. H. Shanks, *ChemSusChem* **2011**, *4*, 1629.
[36] T. Faravelli, A. Frassoldati, G. Migliavacca, E. Ranzi, *Biomass Bioenergy* **2010**, *34*, 290.
[37] B. R. Hough, D. T. Schwartz, J. Pfaendtner, *Ind. Eng. Chem. Res.* **2016**, *55*, 9147.
[38] J. Wang, X. Ku, J. Lin, S. Yang, *Energy Fuels* **2021**, *35*, 10035.
[39] C. Guizani, S. Valin, J. Billaud, M. Peyrot, S. Salvador, *Fuel* **2017**, *207*, 17.
[40] C. Gorton, R. Kovac, J. Knight, T. Nygaard, *Biomass* **1990**, *21*, 1.
[41] D. Humbird, A. Trendewicz, R. Braun, A. Dutta, *ACS Sustainable Chem. Eng.* **2017**, *5*, 2463.
[42] B. H. Caudle, M. B. Gorensek, C. C. Chen, *J. Adv. Manuf. Process.* **2020**, *2*, e10031.
[43] R. Xing, W. Qi, G. W. Huber, *Energy Environ. Sci.* **2011**, *4*, 2193.

[44] M. J. Antal, M. Grønli, *Ind. Eng. Chem. Res.* **2003**, *42*, 1619.

[45] T. Kan, V. Strezov, T. J. Evans, *Renewable Sustainable Energy Rev.* **2016**, *57*, 1126.

[46] R. Ragucci, P. Giudicianni, A. Cavaliere, *Fuel* **2013**, *107*, 122.

[47] V. Dhyani, T. Bhaskar, *Renewable Energy* **2018**, *129*, 695.

[48] P. Kaushal, R. Tyagi, *Renewable Energy* **2017**, *101*, 629.

[49] I. Adeyemi, I. Janajreh, *Renewable Energy* **2015**, *82*, 77.

[50] E. Ranzi, P. E. A. Debiagi, A. Frassoldati, *ACS Sustainable Chem. Eng.* **2017**, *5*, 2867.

[51] M. Henze, M. C. van Loosdrecht, G. A. Ekama, D. Brdjanovic, *Biological Wastewater Treatment*, IWA Publishing, London, UK **2008**.

[52] J. A. Roels, *J. Chem. Technol. Biotechnol.* **1982**, *32*, 59.

[53] W. Gujer, *Systems Analysis for Water Technology*, Springer Science & Business Media, New York **2008**.

[54] C. Ellens, R. Brown, *Bioresour. Technol.* **2012**, *103*, 374.

[55] A. Shoaib, R. El-Adly, M. Hassanean, A. Youssry, A. Bhran, *Egypt. J. Pet.* **2018**, *27*, 1305.

[56] A. Pattiya, S. Sukkasi, V. Goodwin, *Energy* **2012**, *44*, 1067.

[57] C. Di Blasi, *Prog. Energy Combust. Sci.* **2008**, *34*, 47.

[58] A. Sharma, V. Pareek, D. Zhang, *Renewable Sustainable Energy Rev.* **2015**, *50*, 1081.

[59] S. Xiu, A. Shahbazi, *Renewable Sustainable Energy Rev.* **2012**, *16*, 4406.

[60] C. Dupont, L. Chen, J. Cances, J.-M. Commandre, A. Cuoci, S. Pierucci, E. Ranzi, *J. Anal. Appl. Pyrolysis* **2009**, *85*, 260.

[61] M. Calonaci, R. Grana, E. Barker Hemings, G. Bozzano, M. Dente, E. Ranzi, *Energy Fuels* **2010**, *24*, 5727.

[62] J. F. Peters, S. W. Banks, A. V. Bridgwater, J. Dufour, *Appl. Energy* **2017**, *188*, 595.

[63] R. S. Miller, J. Bellan, *Combust. Sci. Technol.* **1997**, *126*, 97.

[64] M. Puig-Arnavat, J. C. Bruno, A. Coronas, *Renewable Sustainable Energy Rev.* **2010**, *14*, 2814.

[65] A. G. Adeniyi, J. O. Ighalo, F. A. Aderibigbe, *SN Appl. Sci.* **2019**, *1*, 1.

[66] J. F. Peters, D. Iribarren, J. Dufour, presented at 21st European Biomass Conf. and Exhibition, Copenhagen, Denmark, June 2013.

[67] R. J. Wooley, V. Putsche, *Development of an ASPEN PLUS physical property database for biofuels components* (No. NREL/TP-425-20685). **1996**, https://doi.org/10.2172/257362.

[68] M. B. Gorensek, R. Shukre, C.-C. Chen, *ACS Sustainable Chem. Eng.* **2019**, *7*, 9017.

[69] F. A. Aly, L. L. Lee, *Fluid Phase Equilib.* **1981**, *6*, 169.

[70] K. S. Pitzer, D. Z. Lippmann, R. Curl Jr., C. M. Huggins, D. E. Petersen, *J. Am. Chem. Soc.* **1955**, *77*, 3433.

[71] J. Boston, P. Mathias, in *Proc. of the 2nd Int. Conf. on Phase Equilibria and Fluid Properties in the Chemical Process Industries*, American Institute of Chemical Engineers, DECHEMA, Berlin **1980**.

[72] W. Zhao, L. Xia, X. Cao, R. Bi, S. Xiang, *Chemical Engineering Transactions* **2020**, *81*, 547.

[73] W. Zhao, X. Sun, L. Xia, S. Xiang, *Ind. Eng. Chem. Res.* **2018**, *57*, 12602.

[74] Aspen Plus (Version 10.0), Aspen Technology, Aspen Plus Inc., Burlington, MA **2017**.

[75] E. Situ, *Energy Efficiency and Renewable Energy*, US Department of Energy Bioenergy Technologies Office, Washington, DC **2015**.

[76] F. Taylor, C. Mullen, A. McAloon, A. A. Boateng, presented at 2008 AIChE Annual Meeting, Philadelphia, PA, November 2008.

[77] J. R. Van Ommen, W. de Jong, *Biomass as a Sustainable Energy Source for the Future: Fundamentals of Conversion Processes*, John Wiley & Sons, Hoboken, NJ **2014**.

[78] A. Trendewicz, R. Braun, A. Dutta, J. Ziegler, *Fuel* **2014**, *133*, 253.

[79] H. Yang, R. Yan, H. Chen, D. H. Lee, C. Zheng, *Fuel* **2007**, *86*, 1781.

[80] A. Dieguez-Alonso, A. Anca-Couce, N. Zobel, F. Behrendt, *Fuel* **2015**, *153*, 102.

[81] T. Bridgeman, J. Jones, I. Shield, P. Williams, *Fuel* **2008**, *87*, 844.

[82] L.-H. Cheng, C.-F. Yeh, K.-C. Tsai, P.-F. Lee, T.-P. Tseng, L.-J. Huang, S.-H. Yeh, H.-T. Hsu, C.-H. Lin, C.-H. Lai, *Fuel* **2019**, *235*, 933.

[83] M. Abou Rjeily, F. Cazier, C. Gennequin, J. H. Randrianalisoa, *Waste Biomass Valoriz.* **2022**, *14*, 325.

[84] J. Park, Y. Lee, C. Ryu, Y.-K. Park, *Bioresour. Technol.* **2014**, *155*, 63.

[85] E. Fernandez, L. Santamaria, M. Amutio, M. Artetxe, A. Arregi, G. Lopez, J. Bilbao, M. Olazar, *Energy* **2022**, *238*, 122053.

[86] F. Shafizadeh, Y. Lai, *J. Organomet. Chem.* **1972**, *37*, 278.

[87] Y. Liao, H. Zhou, *PhD Thesis*, ZheJiang University (Hangzhou, China), **2003**.

[88] T. Hosoya, H. Kawamoto, S. Saka, *J. Anal. Appl. Pyrolysis* **2008**, *83*, 64.

[89] V. Agarwal, P. J. Dauenhauer, G. W. Huber, S. M. Auerbach, *J. Am. Chem. Soc.* **2012**, *134*, 14958.

[90] K. B. Ansari, J. S. Arora, J. W. Chew, P. J. Dauenhauer, S. H. Mushrif, *Energy Fuels* **2018**, *32*, 6008.

[91] K. B. Ansari, J. S. Arora, J. W. Chew, P. J. Dauenhauer, S. H. Mushrif, *Ind. Eng. Chem. Res.* **2019**, *58*, 15838.

[92] A. D. Paulsen, M. S. Mettler, P. J. Dauenhauer, *Energy Fuels* **2013**, *27*, 2126.

SUPPORTING INFORMATION

Additional supporting information can be found online in the Supporting Information section at the end of this article.